JPE 18-6-15

https://doi.org/10.6113/JPE.2018.18.6.1771
ISSN(Print): 1598-2092 / ISSN(Online): 2093-4718

Model Predictive Control for Tram Charging and Its Semi-Physical Experimental Platform Design

Chujia Guo*, Aimin Zhang*, and Hang Zhang†

*School of Electronic and Information Engineering, Xi'an Jiaotong University, Xi'an, China
†School of Electrical Engineering, Xi'an Jiaotong University, Xi'an, China

Abstract

Modern trams with a super capacitor have gained a lot of attention in recent years due to its reliability, convenience, energy conservation and environmental friendliness. Because of its special charging characteristic, the traditional charging structure and control strategy cannot satisfy its charging requirements. This paper presents a new charging topology for fast charging modern trams with a super capacitor and it designs a controller using continuous control set model predictive control (CCS-MPC). There are three contributions in this paper. First, a new charging structure is designed and its mathematics model is derived. The cascade structure is adopted instead of the parallel structure to simplify the control process and to keep the rated power of the controllable part low. Second, a MPC control strategy is proposed to satisfy the charging characteristic. The optimal control signal can be obtained by solving the designed optimization problem. The optimal control signal is related to the discrete control action. In addition, mapping between the continuous control signal and the discrete control action is designed. Third, a semi-physical experimental platform is built to verify the proposed topology and control method. The simulation model and experiment platform are built to verify the correctness of the new structure and its control method. The results obtained show that the new topology can work effectively.

Key words: Continuous control set model predictive control (CCS-MPC), Semi-physical experimental, Tram charging

I. INTRODUCTION

The modern tram is a sustainable method of transportation that has gained a lot of attention because it is reliable, convenient, comfortable, energy efficient and environmentally friendly [1], [2]. Overhead and underground lines used to be the most popular choices for traditional trams with an uninterruptible power supply system. This kind of traditional tram has many limitations and cannot satisfy the transportation requirements of a modern city. Nowadays, thanks to the development of super capacitors, the 'enter and charging' mode has appeared. The 'enter and charging' mode means that the tram only charges when it enters the station. As a result, there are no lines installed in the roads. The charging characteristic of a tram based on a super capacitor is totally different from that of traditional vehicles with energy storage systems. As a result, the charging system needs more attention. The study of charging systems can be divided into two areas, the charging structure and the control strategy [3]. The achievements can be summarized as follows.

A lot of charging structures have been proposed in recent years. A parallel structure was proposed in [4]. The rate power and the charging speed are increased by the proposed structure. However, the rate voltage of each sub-model must be higher to ensure that there is enough of a safety margin, which results in a higher cost. Voltage balance is another important problem of parallel structures. The transfer efficiency is decreased due to the circulating current caused by voltage unbalance. The unbalanced problem needs to be considered in parallel structures. As a result, the control process becomes more complicated. Two charging ports are designed in some structures to avoid conflicts between two trams from different directions. The two charging ports share a common power supply system, which may result in a higher rated power and a higher production cost. The charging systems with energy storage cells mentioned in [5] and [6] are useful for the traditional trams based on a battery. However,

Manuscript received Jun. 2, 2017; accepted Jul. 22, 2018
Recommended for publication by Associate Editor Jaehong Kim.
†Corresponding Author: zhangh@mail.xjtu.edu.cn
Tel: +86-29-8266-8665(ext.167), Xi'an Jiaotong University
*Sch. of Electronic and Information Eng., Xi'an Jiaotong Univ., China

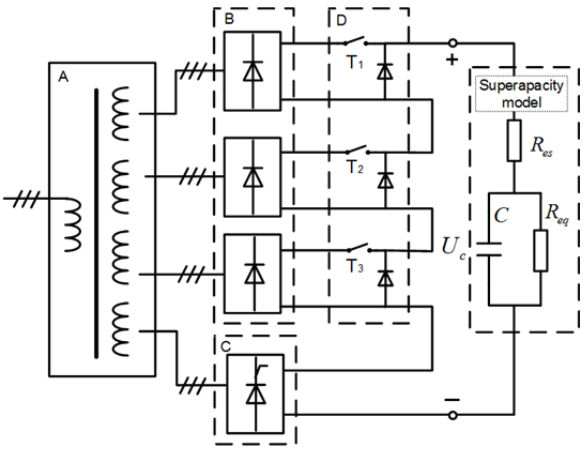

Fig. 1. Proposed structure.

these methods are not suitable for the 'enter and charging' mode of the modern trams based on a super capacitor. All the mentioned structures have a common defect. The sub-modules in these topologies are controllable converters, and each of the controllable sub-modules works under a high voltage condition. This may cause some problems. On the one hand, there are too many controlled variables in the system, which results in the need for a more complicated control algorithm. On the other hand, the high working voltage level of the controllable parts decreases the reliability of the system and increases the cost.

Almost all of the recent charging structures are designed for traditional trams based on a battery. These structures cannot totally satisfy the requirements of emerging modern trams with the 'enter and charging' mode. In this paper, a new charging topology is proposed to decrease the number of controllable device and to simplify the control strategy.

Different charging structures need different control strategies. Modern trams with a super capacitor need a special controller. In the last decade, control strategies have been mainly designed for the traditional trams based on batteries. The charging control methods for electrical vehicles can be divided into two categories. They are charging only and vehicle to grid (V2G). Some interesting ideas which can guide the study of modern trams in this paper are shown in these recent control strategies. The key points of the control method are modeling and optimization.

A small signal model has been deduced in [7] to build a dual loop controller (an inner loop for the current and an outer loop for the voltage). Reference [8] proposed a model of the load structure. The number of electric vehicles (EVs) and the related charging times are considered in the model to reduce the power loss when the load is changed. The methods mentioned before are model based control methods. The model of the charging process is built, and the main problems can be easily solved based on the proposed model. Optimization problems are often extracted in cooperation charging problems [9], [10]. An optimization problem is built in [11] to minimize charging loss. Optimization methods have become a lot more popular in recent years, since almost every technology index can be easily covered by designed objective functions without changing the control structure. For modern trams, the charging time, voltage, power loss and power quality make up the main technology index.

Model predictive control (MPC) is often chosen in the process industry, since it has been in use for decades. MPC shows a perfect dynamic response since predictive values are used to compensate the system delay. In addition, the control process of MPC is easy to understand. Actually, MPC has already been used to solve the charging problems of vehicles, such as fuel efficiency optimization [12] and charging schedule design [13]. For new modern trams, MPC can realize device control and can satisfy the system technology index. However, recent MPC methods are focused on system optimal scheduling and energy optimization [14], [15]. It is difficult to find a suitable control method for modern tram charging process control. In this paper, a controller based on MPC will be designed for the new charging topology.

Based on the aforementioned consideration, a fast charging structure and its control algorithm are proposed in this paper. There are four advantages in this proposed structure and control method.

1) There is no unbalanced condition among different modules, and the circulating problems no longer need to be considered.
2) The output voltage can increase continually from any initial value, and perfect harmonic performance is given by the 24-pulse structure.
3) The controllable part in the designed structure works under a low voltage condition. As a result, the reliability of the system is increased.
4) Because there is only one controllable part, the proposed MPC control strategy is easy to understand. In addition, an explicit control law can be computed offline to reduce the online calculation burden, which results in a fast dynamic response.

A semi-physical experimental platform is built to verify the new structure and its control strategy.

The rest of the paper is divided into five parts, which can be detailed as follows. In section II, the new structure and its working process are described. Section III presents the control system and calculation of the explicit control law. Simulation results are shown in section IV. In section V, a semi-physical experimental platform is built for experimentation. Finally, some conclusions and suggestions for future work are expounded in section VI.

II. Structure and Working Process

The new structure proposed in this paper is shown in Fig. 1. This structure includes three uncontrollable rectifiers and one

controllable rectifier. The whole structure can be divided into four parts based on their function. They are marked A, B, C and D in Fig. 1.

The first part is marked A in Fig. 1. It is the transformer model. A suitable input voltage can be provided by the transformer. The seconded part is marked B in Fig. 1. It consists of three uncontrollable rectifiers to realize step changes of the output voltage. The third part is marked C in Fig. 1. It is a controllable rectifier to realize continuous changes of the output voltage. The last part is marked D in Fig. 1. It is function model. The function model is used to decide whether the related uncontrollable rectifier is enabled or not. The super capacity model in Fig. 1 is established based on the real object.

The initial voltage of the super capacitor is different every time the tram enters a station. Therefore, the charging system needs to provide a suitable initial voltage. According to different initial voltages, the working condition can be divided into four parts. Assume that the fully charged voltage is $4 \cdot U_{part}$. The four working condition is defined as follow:

a. Only the controllable rectifier is switched on, and the initial voltage u_{init} is $0 < u_{init} < U_{part}$.
b. The controllable rectifier and one uncontrollable rectifier are switched on, and the initial voltage u_{init} is $U_{part} < u_{init} < 2 \cdot U_{part}$.
c. The controllable rectifier and two uncontrollable rectifiers are switched on, and the initial voltage u_{init} is $2 \cdot U_{part} < u_{init} < 3 \cdot U_{part}$.
d. The controllable rectifier and three uncontrollable rectifiers are switched on, and the initial voltage u_{init} is $3 \cdot U_{part} < u_{init} < 4 \cdot U_{part}$.

The current loops are shown in Fig. 2. When $0 < u_{init} < U_{part}$, situation a) will be selected. First, T_1, T_2 and T_3 switch off to bypass all of the uncontrollable rectifiers, and only the controllable rectifier is switched on. The fire angle α is $0 < \alpha < 180°$. During this period, the output voltage increased from u_{init} to U_{part} as the fire angle decreased to $0°$. When the output voltage reaches U_{part}, situation b) occurs. Keep T_1 and T_2 off, and T_3 on. The fire angle is equal to $180°$. At this instant, the current loop is changed. However, the output voltage is still kept at U_{part}, and it increases from U_{part} to $2 \cdot U_{part}$ during situation b). Situations c) and d) are the same as a) and b). Under these two situations, the output voltage increased from $2 \cdot U_{part}$ to $3 \cdot U_{part}$ and from $3 \cdot U_{part}$ to $4 \cdot U_{part}$, respectively. These four situations can make the output voltage continuously increase from u_{init} to $4 \cdot U_{part}$.

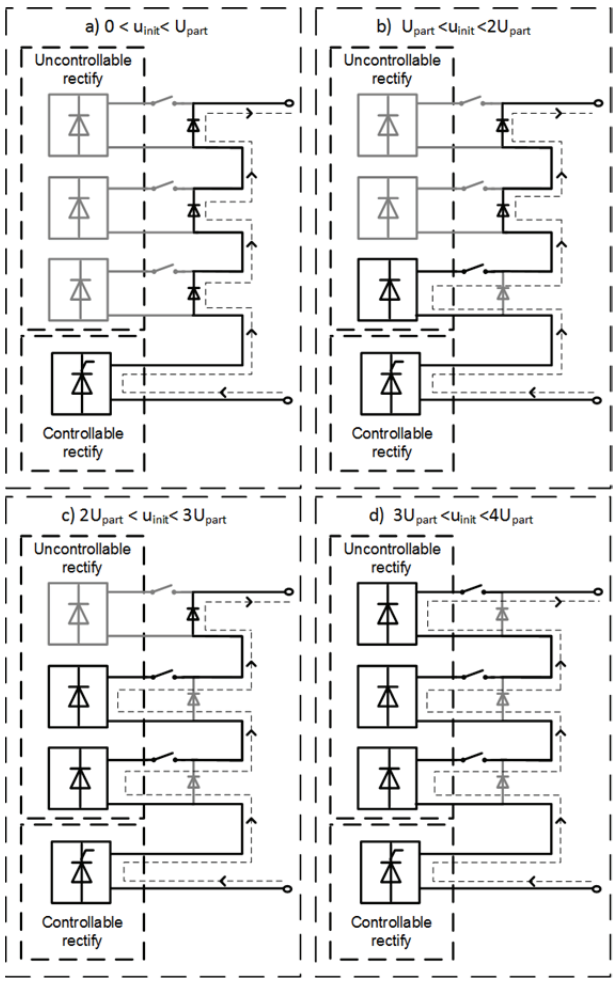

Fig. 2. Working process with different current loops.

Based on the working process illustrated above, it is obviously that the output voltage is designed to increase continually from any initial value. The controllable part in this structure only supplies a quarter of the voltage of the system, which makes the system more reliable.

III. MPC OF THE CHARGING STRUCTURE

A. Output Voltage Calculation

The proposed topology consists of two different types of power electronic devices (uncontrollable rectifiers and a controllable rectifier). The output voltage can be deduced by calculating the rectifiers. The formulation between the input and output of the uncontrollable rectifiers is shown in equation (1).

$$U_{unctr} = 2.34 \sim 2.45 U_2 \tag{1}$$

Where, U_2 is the RMS (root mean square) value of the line voltage of the AC (alternating current) system.

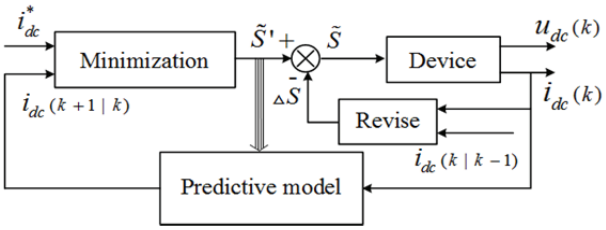

Fig. 3. Block diagram of the control method.

The output voltage of the controllable rectifier (U_{ctr}) is controlled by the fire angle α, which is shown in equation (2).

$$U_{ctr}=\frac{1}{\pi/3}\int_{\frac{\pi}{3}+\alpha}^{\frac{2\pi}{3}+\alpha}\sqrt{6}U_2\sin\omega td(\omega t)=2.34U_2\cos\alpha \quad (2)$$

There are three uncontrollable rectifiers and one controllable rectifier in the new structure, and the uncontrollable rectifiers can be controlled by T_1, T_2, T_3. Value 1 shows that the rectifiers are switched on (T_i=1, $i=1,2,3$), and value 0 shows that the rectifiers are bypassed (T_i=0, $i=1,2,3$). T_i (i=1,2,3) can be reflected to a continuous signal $\tilde{S}$ by denoting $\tilde{S}=T_1+T_2+T_3+\cos\alpha$. The output voltage of the system is shown in equation (3).

$$\begin{aligned}U_{dc}&=U_1+U_2+U_3+U_4\\&=(T_1+T_2+T_3+\cos\alpha)\cdot 2.34U_2\\&=\tilde{S}\cdot 2.34U_2\end{aligned} \quad (3)$$

Where, T_1, T_2, T_3=1 or 0.

B. Control Strategy

The control strategy is important because it directly influences the charging performance. Because the model of the charging structure can be easily obtained and the control problem can be summarized as an optimization problem, the model predictive control method is designed to realize a constant current charging process. There are three typical elements of the model predictive control method, the model, the cost function and the optimization procedure.

The predictive model plays an important role in the realization of the MPC, which needs to present the dynamic characteristics of the process, predict future outputs of the system and be easily understood. The function of the model is predicting the output $\hat{y}(t+k|t)$ at future instants t+1 based on known information at instant t.

In order to obtain a suitable model for the charging system, an equivalent circuit of the super capacitor equipped in the tram is given in Fig. 1. Considering the charging characteristics of super capacitor, the parameters of this equivalent circuit are defined as follow: $R_{eq}=10\text{K}\Omega$, $R_{es}=10\text{m}\Omega$ and $C=7.5\text{F}$.

The output voltage is shown as follows:

$$\frac{\mathrm{d}u_c}{\mathrm{d}t}=\frac{2.34u_2\tilde{S}}{R_{es}C}-\frac{(R_{es}/R_{eq}+1)}{R_{es}C}u_c \quad (4)$$

$$u_{dc}=\left[C\frac{\mathrm{d}u_c}{\mathrm{d}t}+\frac{u_c}{R_{eq}}\right]R_{es}+u_c \quad (5)$$

The discrete model can be obtained by the Euler method:

$$\begin{aligned}u_c(n+1)&=u_c(n)\\&+T_s\left[\frac{2.34u_2\mathrm{sum}(S)}{R_{es}C}-\frac{(R_{es}/R_{eq}+1)}{R_{es}C}u_c(n)\right]\end{aligned} \quad (6)$$

Where, T_s is the control period. A discrete model of the output current has to be obtained because the current is the main feedback variable. It can be easily obtained from equation (6).

$$\begin{aligned}i(n+1)&=\frac{u_{dc}-u_c(n+1)}{R_{es}}\\&=\frac{u_{dc}-u_c(n)-T_S\left[\frac{u_{dc}(n)}{CR_{es}}-\frac{(R_{es}+R_{eq})}{CR_{es}R_{eq}}u_c(n)\right]}{R_{es}}\end{aligned} \quad (7)$$

The selectable cost function is multitudinous. For the current constant charging process, the output current i_{dc} is fixed to the reference current i_{dc}^*, and the voltage u_{dc} gradually gets close to the reference u_{dc}^*. When u_{dc} is almost equal to u_{dc}^*, the current decreases and the voltage is kept constant. The cost function is designed as equation (8) [16]. The output current, switching frequency, switching dissipation and power quality of the AC side are all important factors [17]. However, in this paper, only the current has been considered to realize the basic charging process.

$$F=\left(i_c^*-i_c\right)^2 \quad (8)$$

In order to reduce the computational burden and to ensure better preference, many algorithms have been proposed to reduce computation complexity [18], [19]. In this paper, the control signal $\tilde{S}$ defined in equation (8) is a continuous signal, which is related to discrete control actions. The creation of $\tilde{S}$ turns the hybrid control system into a simple continuous control set model predictive control system. It also simplified the complicated computation. When solving the optimization problem, the constraint of the cost function is the limitation of the control signal. The feasible region of the control signal $\tilde{S}$ is shown in equation (9), which is denoted as S_{CCM}.

$$\tilde{S}\in[0,4] \quad (9)$$

The control signal $\tilde{S} \in [0,4]$ is kept constant in one control period $t_k \le t < t_{k+1}$. The definition of $\tilde{S}$ is used to transform the discrete problem to a continuous problem, which is used to solve the original non-convex optimal problem. The trace of the discrete system is dense in the trace of the new continuous system.

An embedded PI can be defined as:

$$J(t_0,t_f,u_{c0},u_{dc0},\tilde{S}) = \int_{t_0}^{t_f} \left[\tilde{S}(t) \cdot F(t,i_c) \right] dt \tag{10}$$

Where, $F \in C$ defines the current tracking performance. $t \in \left[t_0, t_f \right]$ is the finite time domain of the optimal process. The calculation interval (control period) T_s is related to t_0 and t_f. u_{c0} and u_{dc0} are the initial values of u_c and u_{dc}, which are defined as $u_c(t_0) = u_{c0}$ and $u_{cd}(t_0) = u_{cd0}$.

The embedded optimal control problem in each period is shown in equation (11).

$$\min_{S \in S_{CCM}} J\left(t_0,t_f,u_{c0},u_{dc0},\tilde{S}\right) \tag{11}$$

Obviously, the solution of this problem exists because the feasible region S_{CCM} is not empty, compact and convex. The problem proposed in equation (11) can be solved. An explicit control law $\tilde{S}$ can be computed beforehand.

$$\tilde{S}_k(n+1) = \frac{\frac{T_s u_{dc}}{CR_{es}} \cdot \frac{2.34u_2}{R_{es}} + \left[\frac{1}{R_{es}} + \frac{T_s(R_{eq}+R_{es})}{CR_{eq}R_{es}} \right] u_c(n)}{\frac{2.34u_2}{R_{es}}} \tag{12}$$

From the known continuous control law $\tilde{S}_k$, the control action can be obtained by using the mapping algorithm shown in equation (13).

$$\begin{cases} \text{when } 0 < \tilde{S}_k < 1, \ T_1 = T_2 = T_3 = 0, \cos\alpha = \tilde{S}_k, \\ \text{when } 1 < \tilde{S}_k < 2, \ T_1 = 1, T_2 = T_3 = 0, \cos\alpha = \tilde{S}_k - 1, \\ \text{when } 2 < \tilde{S}_k < 3, \ T_1 = T_2 = 1, T_3 = 0, \cos\alpha = \tilde{S}_k - 2, \\ \text{when } 3 < \tilde{S}_k < 4, \ T_1 = T_2 = T_3 = 1, \cos\alpha = \tilde{S}_k - 3, \end{cases} \tag{13}$$

The structure of the MPC is shown in Fig. 3. The designed controller is for the current constant charging mode. Therefore, the reference is a constant current value i_{dc}^*. i_{dc}^* and i_{dc} are sent to the minimization part to calculate the control signal $\tilde{S}'$. The control signal $\tilde{S}'$ needs to be regulated by ΔS from the revised part based on the current value at the time instant k ($i_{dc}(k)$) and the predictive value at the time instant k-1 ($i_{dc}(k \mid k-1)$). Finally, control action $\tilde{S}'$ is used to obtain an optimal output.

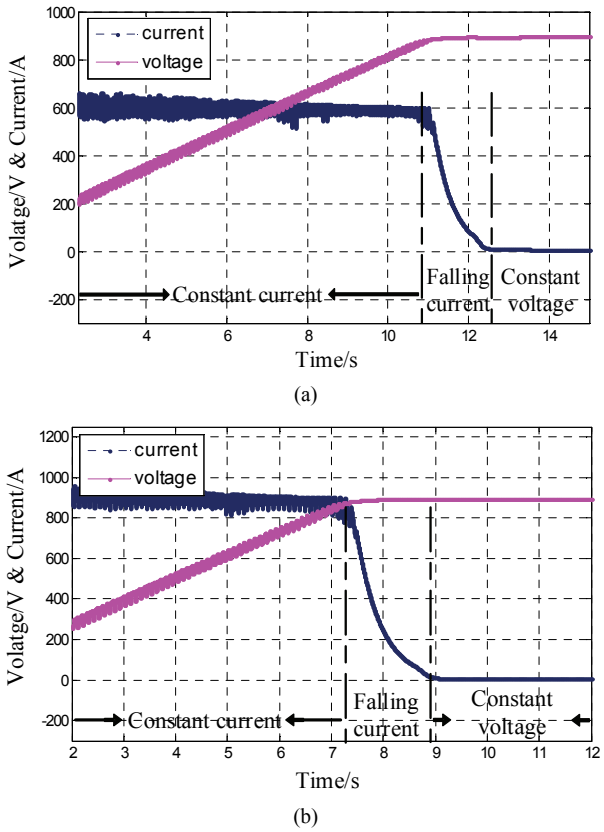

Fig. 4. Simulation results: (a) 900A charging current case; (b) 600A charging current case.

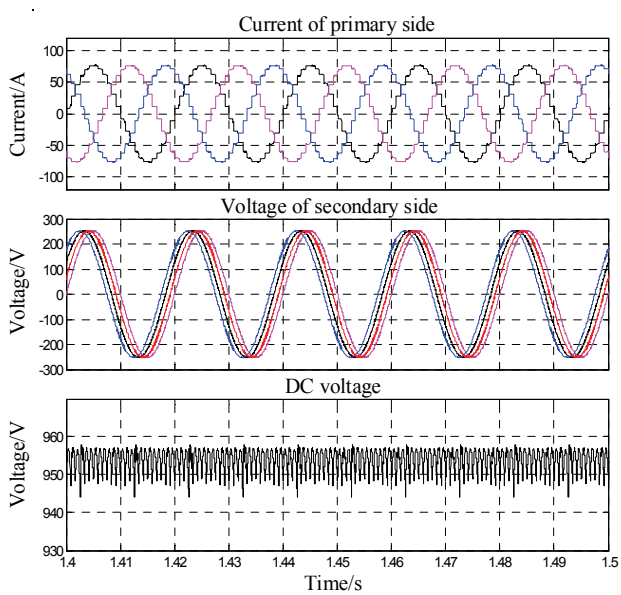

Fig. 5. Voltage and current curves of the charging process with a 900A charging current.

Based on the proposed control method, the predictive values of the system state are used. This results in a fast dynamic performance. At the same time, the optimal control action is computed offline which is a lot more suitable for hardware realization.

TABLE I
HARMONIC CONTENT OF CURRENT IN PRIMARY WINDING

Frequency	Content
50Hz (Fnd)	99.52%
150Hz (h5)	0.08%
350Hz (h7)	0.08%
550Hz (h11)	0.08%
650Hz (h13)	0.08%
850Hz (h17)	0.08%

IV. SIMULATIONS

In order to verify the correctness of the topology and the control strategy, a MATLAB/SIMULINK model has been established. The current constant charging processes for a tram are simulated and harmonic content has been analyzed.

A. Current Constant Charging Processes

The simulation in this part used the MPC controller designed in this paper to realize the charging processes. Two charging processes with different charging current are shown in this part. The main parameters in this simulation are defined as follow: the voltage source, capacitance and voltage reference are 10KV, 7.5F and 900V, respectively.

The charging processes with different current references are shown in Fig. 4(a)-(b). The current referents are $900\mathrm{A}$ and $600\mathrm{A}$, respectively. There are three periods of each charging process, current constant, current decrease and voltage constant. The charging time known from simulation results are $7.5\mathrm{s}$ and $11\mathrm{s}$ for the case of $900\mathrm{A}$ and $600\mathrm{A}$, which is close to theoretical value calculated by $t = CU / I$.

B. Harmonic Analysis

Not considering charging the voltage and charging current, the harmonic content also an important technology index. The charging device needs to reduce harmonic distortions. The structure in this paper has a 24-pulse structure to reducing the harmonic distortions. In this part, the harmonic content of the AC current is analyzed under the maximum voltage output situation. Fig. 5 presents the voltage of the primary and secondary side of the transform and the output DC voltage.

Because of its 24-pulse structure, the current of the ac side shows 24-step waves in one period. The DC voltage also shows a 24-pulse characteristic. Theoretically, this gives a better performance than that of a 6-puls structure without a phase shift transformer. Table I presents quantitative analysis results of the current of primary side using a FFT tool.

V. EXPERIMENTS

The use of a semi-physical experiment is a new choice for electrical experiment, and it is accepted by more and more people because it has a high flexibility and fidelity. It is suitable for the testing of complicated power systems and control algorithms [20], [21]. In this part, a semi-physical experimental platform is built to verify the proposed topology and control algorithm. The minimum sampling frequency of the experiment platform is 12 kHz, which is suitable for a lot of the electrical experiments. The experimental platform includes a real-time computing unit, I/O terminals, communication part (IEC61950) and physical control part. A close loop is formed using the I/O unit to send real-time measurement signals back to an IPC (Industrial Personal Computer) to determine the next control action. The detecting voltage and current signals sent to the control panel are real signals that are equal to the signals from a real power system. Fig. 6(a)-(b) depict the basic structure and the experimental platform.

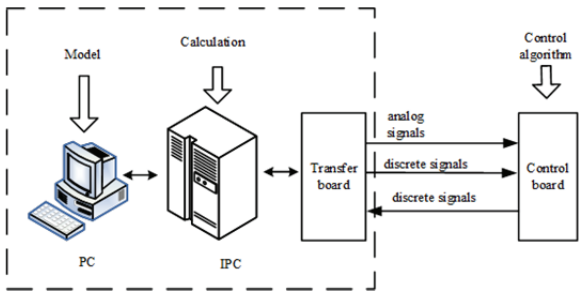

(a)

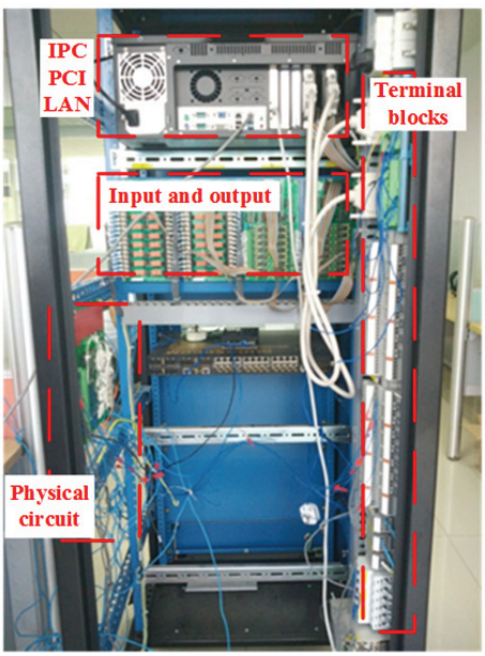

(b)

Fig. 6. Semi-physical simulation platform: (a) Structure diagram; (b) Electrical cabinets.

The platform is composed of three parts, an IPC, input and output modules and a physical control circuit. Digital signals, analog signals and bland node signals are three different signal types in this system. Therefore, the signals transferred between the physical circuit and the IPC need to be converted several times. The function of each module is shown in Fig. 6(a).

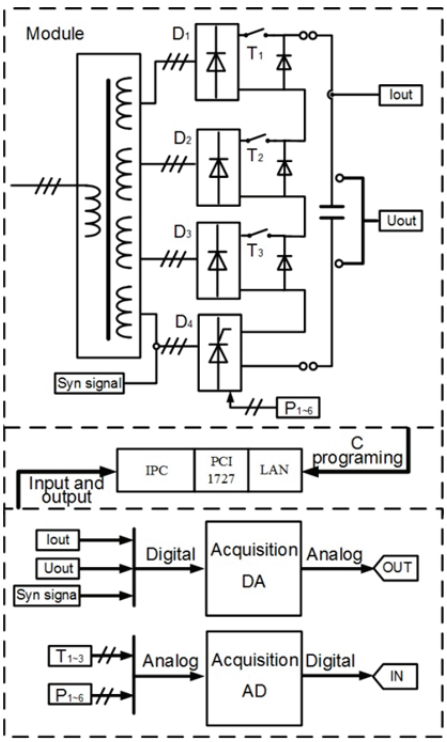

Fig. 7. SIMULINK model.

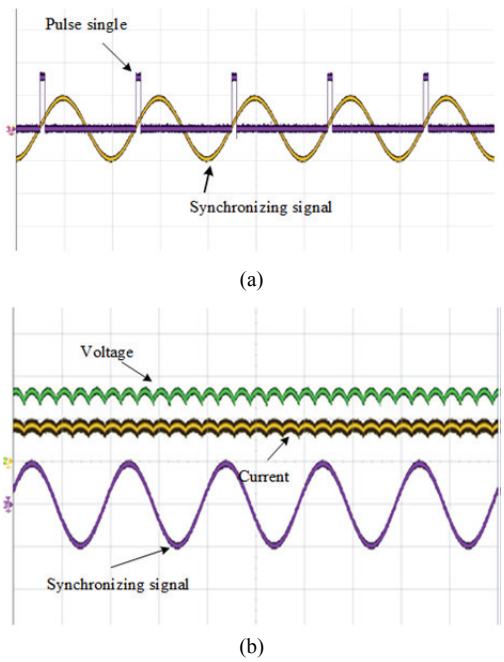

Fig. 8. Experimental results: (a) Synchronizing signal and pulse signal; (b) DC current and DC voltage of the system.

Terminal blocks: output terminals of analog signals, and output and input terminals of discrete signals.

Physical circuit including a transfer board (converts the photosignal produced by control board to blank nodes which are used in the experimental platform) and a control board (physical control system).

The whole experimental platform can be divided into two

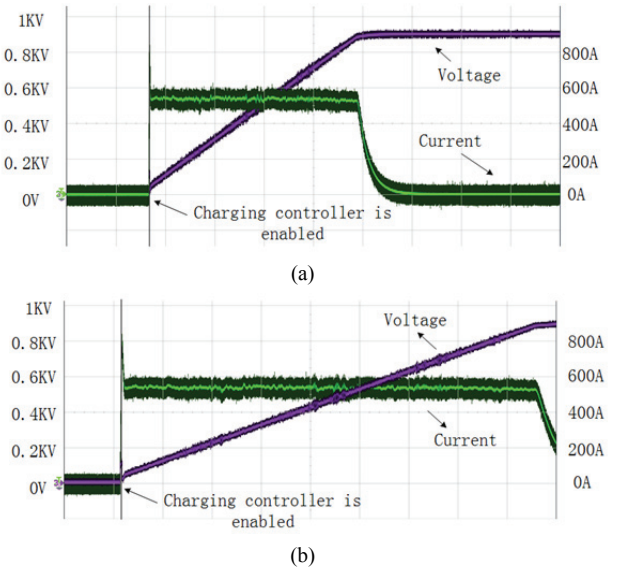

Fig. 9. Experimental results: (a) Whole charging process; (b) Constant current stage.

parts, the real part and the virtual part. The virtual part is a series code compiled in the C programming language based on the SIMULINK module, which is realized by the IPC, to achieve a real time system. The signals from the virtual part are not simulation signals, but real power signals that are equal or proportional to those of a real power electronic device. The control system is physical instrument, which can be directly used as a physical power electronic device. This kind of experiment gives the real working conditions and tests the effectiveness of the controller.

For the charging system, the module for the IPC consists of three analog outputs and nine digital inputs, which are shown in Fig. 7. The charging structure is built and reprogrammed in the C language. The codes are sent to the IPC. According to the designed control method, three signals are necessary for the control process. They are the output current, output voltage and synchronized signal. These signals are transmitted to the control board through output terminals. The output signal can be seen clearly using a scope. The control action obtained from $\tilde{S}$ includes three signals for the uncontrollable rectifies and six signals for the controllable rectifier. These control actions are transmitted through the input terminal (BI).

Fig. 8(a) shows the synchronizing signal and the pulse signal generated by the control board. The output voltage and current are shown in Fig. 8(b).

Experiment results of the charging process are shown in Fig. 9. In this figure, (a) is the whole charging process and (b) presents the constant current stage. When charging begins, the current immediately rises to the reference value, and the voltage is linearly increased. When the voltage reaches the reference, the current quickly decreases.

In order to verify the effectiveness of the proposed topology and the MPC based approach, the system of a traditional

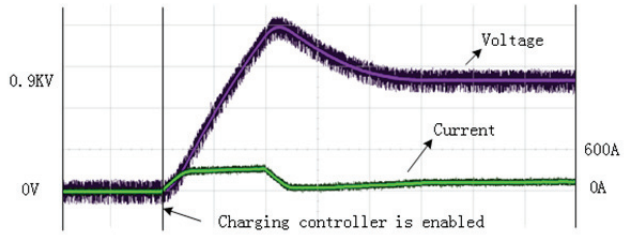

Fig. 10. Experimental result of a traditional system with a PI controller.

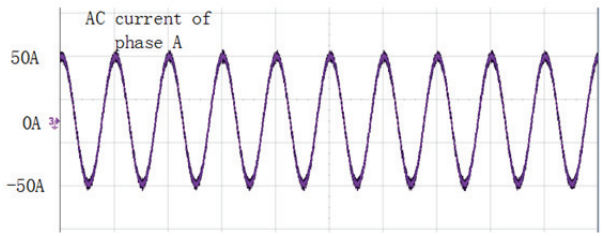

Fig. 11. Experimental result of AC current.

parallel structure with a usual PI controller is realized on the semi-physical experimental platform, and the constant current charging process results are shown in Fig. 10. Obviously, all of the dynamic response performances are worse than those of the results obtained in this paper. The setting time of the current (both the rising process and the declining process) is longer than that of the MPC method. As a result, the response process of the voltage does not show a perfect performance. The setting time is longer and the overshoot is larger.

A waveform of the AC current is shown in Fig. 11. The waveform is obtained during the steady state of the system. It can be seen that the waveform is a standard sinewave without any obviously harmonic pollution.

VI. Conclusions

This paper presented a new charging topology for modern trams that possesses advantages including fewer controllable devices, a simpler control logic and improved reliability. A model predictive current control strategy for current constant charging also presented. The charging current tracked the reference by solving a designed optimal problem in the CCS-MPC. The explicit expression of the control law is calculated beforehand to reduce online computations. Simulation and experimental results reveal that the structure possesses a satisfactory performance and is suitable for modern tram charging. Although the control method achieves a satisfactory performance, the stability of the controller has not be verified. This will be the main focus of future work.

Last but not the least, a semi-physical simulation platform has been built. It was used to test the correctness of the main circuit and the physical control system. Experiment results further prove the reasonability of the proposed structure and the control algorithm. This experimental platform is suitable for experiments on the charging system. It can also be applied to verify the designs of any power electronic structures. It can simplify the research process, reduce the cost of reliability tests, and shorten the development cycle.

References

[1] T. P. Nuca and V. Esanu, "Urban electric vehicles traction: achievements and trends," *Electrical and Power Engineering (EPE)*, pp. 25-27, 2012.

[2] M. Z. Chymera, A. C. Renfrew, M. Barnes, and J. Holden, "Modeling Electrified Transit Systems," *IEEE Trans. Veh. Technol.*, Vol. 59, No. 6, pp. 2748-2756, Jul. 2010.

[3] T. Jakub, S. Lubos, P. Zdenek, and D. Pavel, "Position-based T-S fuzzy power management for tram with energy storage system," *IEEE Trans. Ind. Electron.*, Vol. 62, No. 5, pp. 3061-3071, May 2015.

[4] L. Yunzhi, L. Bing, C. Zhigang, and D. Yanhua, "Power system of modern tram," *China Patent*, 201520328125.7, 2015.

[5] Z. Jinghua, L. Qiupei, and Z. Xiaowei, "A new power supply system for modern tram," *Power and Electron Technology*, Vol. 49, No. 6, pp. 101-103, 2015.

[6] C. Flavio, I. Diego, K. Keiichiro, and F. Luigi, "Line-voltage control based on wayside energy storage systems for tramway networks," *IEEE Trans. Power Electron.*, Vol. 31, No. 1, pp. 884-899, Jan. 2015.

[7] H. Omar, A. M. Mohamed, L. Philippe, and V. M. Joeri, "Modeling and analysis of a hybrid PV/second-Life battery topology based fast DC-charging systems for electric vehicles," *Power Electronics and Applications*, pp. 1-11, 2015.

[8] S. Bo, S. Zhongpei, W. Dajun, and L.Yan, 'Research on optimal control of electric vehicle charging in residential area', *Chinese Control Conference*, pp. 8617-8621, 2016.

[9] T. Roham, S. Catarina, and G. Álvaro, "Development of an algorithm to control and optimize the coordinated charging process of a group of electric vehicles," *Smart System Tech.*, pp. 1-5, 2014.

[10] M. Yuting, X. Hao, F. Minyue, and L. Zhiyun, "Decentralized PWM-based charging control for plug-in electric vehicles," *European Control Conference (ECC)*, pp. 1070-1075, 2015.

[11] T. Yechen, Z. Jin, and B. Math, "Aggregated optimal charging and vehicle-to-grid control for electric vehicles under large electric vehicle population," *IET Gener., Transm. Dist.*, Vol. 10, No. 8, pp. 2012-2018, May, 2016.

[12] K. J. Yu, H. Z. Yang, X. G. Tan, T. Kawabe, Y. Guo, Q. Liang, Z. Fu, and Z. Zheng, "Model predictive control for hybrid electric vehicle platooning using slope information," *IEEE Trans. Intell. Transp. Syst.*, Vol. 17, No. 7, pp. 1894-1909, Jan. 2016.

[13] T. Wanrong and Z. Ying, "A model predictive control approach for low-complexity electric vehicle charging scheduling: Optimality and scalability," *IEEE Power & Energy Society*, Vol. 32, No. 2, pp. 1050-1063, Jun. 2016.

[14] M. Josevski and D. Abel, "Tube-based MPC for the energy management of hybrid electric vehicles with non-parametric driving profile prediction," *American Control Conference*, pp. 623-630, 2016.

[15] J. Tang, L. Guo, B. Gao, Q. Liu, S. Yu, and H. Chen, "Energy management of a parallel hybrid electric vehicle with CVT using model predictive control," *Chinese Control Conference*, pp. 4396-4401, 2016.
[16] J. Rodríguez, J. Pontt, C. Silva, P. Correa, P. Lezana, P. Cortes, and U. Ammann, "Predictive current control of a voltage source inverter" *IEEE Trans. Ind. Electron.*, Vol. 54, No. 1, pp. 495-503, Feb. 2007.
[17] V. Sergio, M. Carlos, B. Carlos, and L. G. Franquelo, "Design and experimental validation of a model predictive control strategy for a VSI with long prediction horizon', *IEEE Conference of Industrial Electronics Society*, pp. 5786-5791, 2013.
[18] A. Bemporad, F. Borrelli, and M. Morari, "Model predictive control based on linear programming," *IEEE Trans. Autom. Contr.*, Vol. 47, No. 12, pp. 1974-1985, Dec. 2002.
[19] A. Bemporad, M. Morari, V. Dua, and E. Pistikopoulos, "The explicit linear quadratic regulator for constrained systems," *Automatica*, Vol. 38, No. 1, pp. 3-20, Jan. 2002.
[20] T. Pengfei, L. Chongru, H. Guowei, Q. Guo, and X. Lin, "Design and Experimental Verification of a Hardware-in-the-loop Simulation Platform for Modularized Multilevel Converter," *Autom. Electric Power Syst.*, Vol. 40, No. 1, pp. 122-127, 2016.
[21] C. Yuehua, H. Qian, J. Bin, "Design and simulation of fault diagnosis based on NUIO/LMI for satellite attitude control systems," *J. Syst. Eng. Electron.*, Vol. 23, No. 4, pp. 581-587, 2012.

Chujia Guo was born in Xi'an, China, in 1989. She received her B.S. and M.S. degrees from the Shaanxi University of Science and Technology, Xi'an, China, in 2011 and 2014, respectively. She is presently working towards her Ph.D. degree in Electrical Engineering at Xi'an Jiaotong University, Xi'an, China. Her current research interests include power electronic converters, renewable energy systems and hybrid ac/dc microgrids.

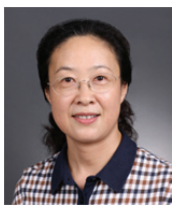

Aimin Zhang received her B.S., M.S. and Ph.D. degrees in Electrical Engineering from Xi'an Jiaotong University, Xi'an, China, in 1983, 1985 and 2008, respectively. She is presently working as a Professor in the School of Electronic and Information Engineering, Xi'an Jiaotong University. Her current research interests include nonlinear control theory and power electronics.

Hang Zhang received his B.S. and M.S. degrees in Electrical Engineering from Xi'an Jiaotong University, Xi'an, China, in 1983 and 1985, respectively. He is presently working as an Assistant Professor in the School of Electrical Engineering, Xi'an Jiaotong University. His current research interests include HVDC transmission systems and power electronics.